



SACOMAR

Technologies for Safe and Controlled Martian Entry

SPA.2010.3.2-04

EU-Russia Cooperation for Strengthening Space Foundations (SICA)

Re-entry Technologies and Tools

Theme 9 - Space

Activity 9.3 - Cross-Cutting-Activities

Area 9.3.2 - International Cooperation

Deliverable Reference Number: D 5.2

Deliverable Title: *Results of experimental study in HEG*

Due date of deliverable: 1st December 2011

Actual submission date: 21st February 2012

Start date of project: 1th January 2011

Duration: 18 months

Organisation name of lead contractor for this deliverable: DLR

Revision #: 0

Project co-funded by the European Commission within the Seventh Framework Programme		
Dissemination Level		
PU	Public	X
PP	Restricted to other programme participants (including the Commission Services)	
RE	Restricted to a group specified by the consortium (including the Commission Services)	
CO	Confidential, only for members of the consortium (including the Commission Services)	

APPROVAL

Title	Issue	Revision
<i>Results of experimental study in the High Enthalpy Shock Tunnel Göttingen (HEG)</i>	1	0

Author(s)	Date
Jan Martinez Schramm	21.2.2012


Approved by	Date
Jan Martinez Schramm 	21.2.2012

Table of Contents

Table of Contents	i
List of figures	ii
List of tables	iii
Acronyms	iv
Nomenclature	v
1 Introduction	1
2 Wind Tunnel Model or Probe	2
2.1 Material	2
2.2 Reference Dimensions and Basic Shape	2
2.3 Instrumentation of the Model	6
3 Experimental Setup	7
3.1 The High Enthalpy Shock Tunnel Göttingen (HEG)	7
3.2 Test Matrix	9
3.3 Free stream conditions	10
4 Experimental Measurement Techniques	13
4.1 Surface Pressure Measurements	13
4.2 Surface Heat Flux Measurements	13
4.3 High Speed Flow Visualisation	13
5 Results	15
5.1 Surface Pressure	16
5.2 Surface Heat Flux	17
5.3 Flow visualisation	19
6 Conclusions	21
7 References	22

List of figures

Figure 1: Sketch of the wind tunnel model.	2
Figure 2: Technical drawing of the wind tunnel model with thermocouple instrumentation.	3
Figure 3: Technical drawing of the wind tunnel model with pressure transducer instrumentation	4
Figure 4: Photos of the pressure probe (left: non instrumented, right: instrumented).	3
Figure 5: Photographs of the probe instrumented with thermocouples (left: outside, middle: inside, right: installed in the test section of HEG.	4
Figure 6: Schematic (left) and photographic views (right) of HEG.	8
Figure 7: Schematic of the optical setup for the high speed flow visualisation. H: Parabolic mirrors, S: Plane mirrors, L: Lenses, A: Focal plane, R: Razor blade.	14
Figure 8: Results of the surface heat flux measurements for all runs..	17
Figure 9: Results of the averaged heat flux measurements..	18
Figure 10: Experimental Schlieren images of the lp condition. The runs are from left to right: 1234, 1235 and 1255.	19
Figure 11: Experimental Schlieren images for the hp condition. The runs are from left to right: 1244, 1245, 1247.	19

List of tables

Table 1: Coordinates of the transducers installed into the model.	6
Table 2: Test matrix of the runs performed.	9
Table 3: Free stream conditions of the four runs performed with the lp condition. Additionally the averages and the repeatability is given at the end of each column.	11
Table 4: Free stream conditions of the five runs performed with the hp condition. Additionally the averages and the repeatability is given at the end of each column	12
Table 5: Results of the pressure measurements.	16

Acronyms

DLR	German Aerospace Center e.V.
HEG	High Enthalpy Shock Tunnel Göttingen
ESTC	Equilibrium Shock Tube Calculation
CEA	Chemical Equilibrium with Applications
NASA	National Aeronautics and Space Administration
SR	Shock Reflection, time when HEG nozzle starts, used to normalize all times in this report
CFD	Computational Fluid Dynamics
WP	Work Package

Nomenclature

Latin Symbols

p	pressure
T	temperature
h	enthalpy
M	Mach number
u	velocity
q	Heat flux
q _d	dynamic pressure, $\frac{1}{2} \rho u^2$

Greek Symbols

ρ	density
γ	ratio of specific heats
μ	viscosity
ξ	mass fraction
σ	standard deviation
η	ratio between Pitot Pressure and dynamic pressure

Subscripts

∞	free stream condition
0	reservoir condition
1	pre shock conditions
2	post shock condition
t	total flow value, also Pitot pressure
ref	reference value use for normalisation

1 Introduction

The main objective of the project “Technologies for **Safe** and **Controlled Martian Entry**” (SACOMAR) is the experimental and numerical study of gas surface interaction phenomena in the high enthalpy flow field behind the bow shock in front of a model at Martian entry flow conditions. The improvement of physical modeling using experimental data and its implementation into the CFD codes is essential to understand and interpret the physical processes. At the end the project will allow to estimate the aero thermal loads on the vehicle more accurately.

This report describes the experiments performed in the High Enthalpy Shock Tunnel Göttingen (HEG) of the German Aerospace Center (DLR). The model used is a probe configuration of a blunt cylindrical shape with a diameter of 100 mm. This configuration has been defined within SACOMAR as a reference shape and all experimental and numerical work focusses on the determination and reconstruction of the flow around this shape.

The report is structured as follows. Chapter 2 beginning on page 2 describes the wind tunnel model for HEG of the SACOMAR configuration to some detail, the chapter 3 beginning on page 7 contains the description of the experimental setup. Here, the HEG facility is described, the free stream conditions used for the experimental testing and all relevant experimental techniques used to obtain the results.

The results are presented in chapter 5 starting on page 15. Here the results for the surface pressure measurements, the surface heat flux measurements and the flow visualizations are described.

A short form summary of all results and some conclusions are given in chapter 6 beginning on page 21.

2 Wind Tunnel Model or Probe

The wind tunnel model was proposed by DLR within the HyFIE project. After the design, the model was manufactured by the DLR Cologne group. After finalization of the manufacturing, the model was delivered to DLR Göttingen. DLR Göttingen instrumented the model with thermocouples in order to determine the surface heat flux during the experiments. Additionally, a second model was designed and manufactured by DLR Göttingen. This model was instrumented with pressure transducers

2.1 Material

The model was manufactured out of stainless steel.

2.2 Reference Dimensions and Basic Shape

The model used within the SACOMAR project is a blunt cylinder with a diameter $D = 100$ mm. The radius from the blunt front side to the cylindrical body is $R = 11.5$ mm. The model or probe is aligned to the flow in such a way, that the streamlines are perpendicular to the axis of the model. The basic geometry of the model and the flow direction is given in Figure 2.

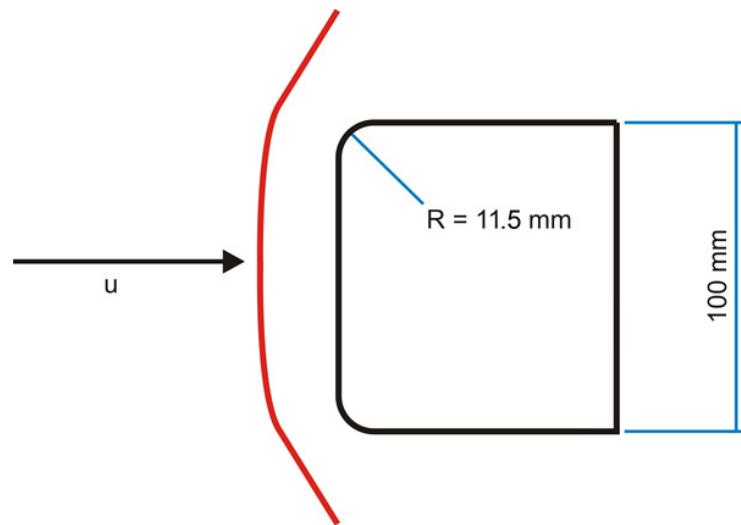


Figure 1: Sketch of the wind tunnel model.

As already described, two models have been manufactured. One model was instrumented with ten thermocouples in a radial direction. The distribution is equally space on one side of the stagnation point and on the other side of the stagnation point. The spacing on one side is 5 mm and on the other side, the spacing is 10 mm. The manufacturing drawing of the model or probe is given in Figure 2 on page 3.

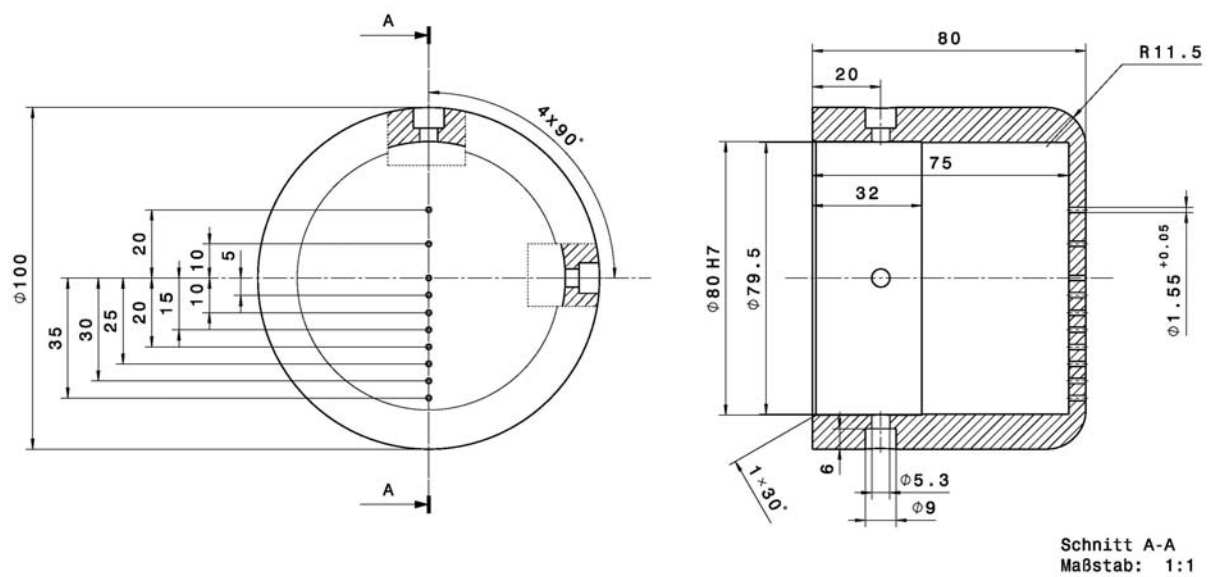


Figure 2: Technical drawing of the wind tunnel model with thermocouple instrumentation.

The model installed with pressure transducers is shown in Figure 4 on page 4. In this figure the technical drawing is given. The pressure transducer model is equipped with seven pressure transducers. One pressure transducer is installed in the stagnation point of the model. The remaining six pressure transducers are positioned on a circle around the stagnation point. The circle has a diameter of 28 mm and therefore a radius of 14 mm. Since the transducers are equally spaced on the circumference, the angle between the pressure transducer taps is 60° .



Figure 3: Photos of the pressure probe (left: non instrumented, right: instrumented).

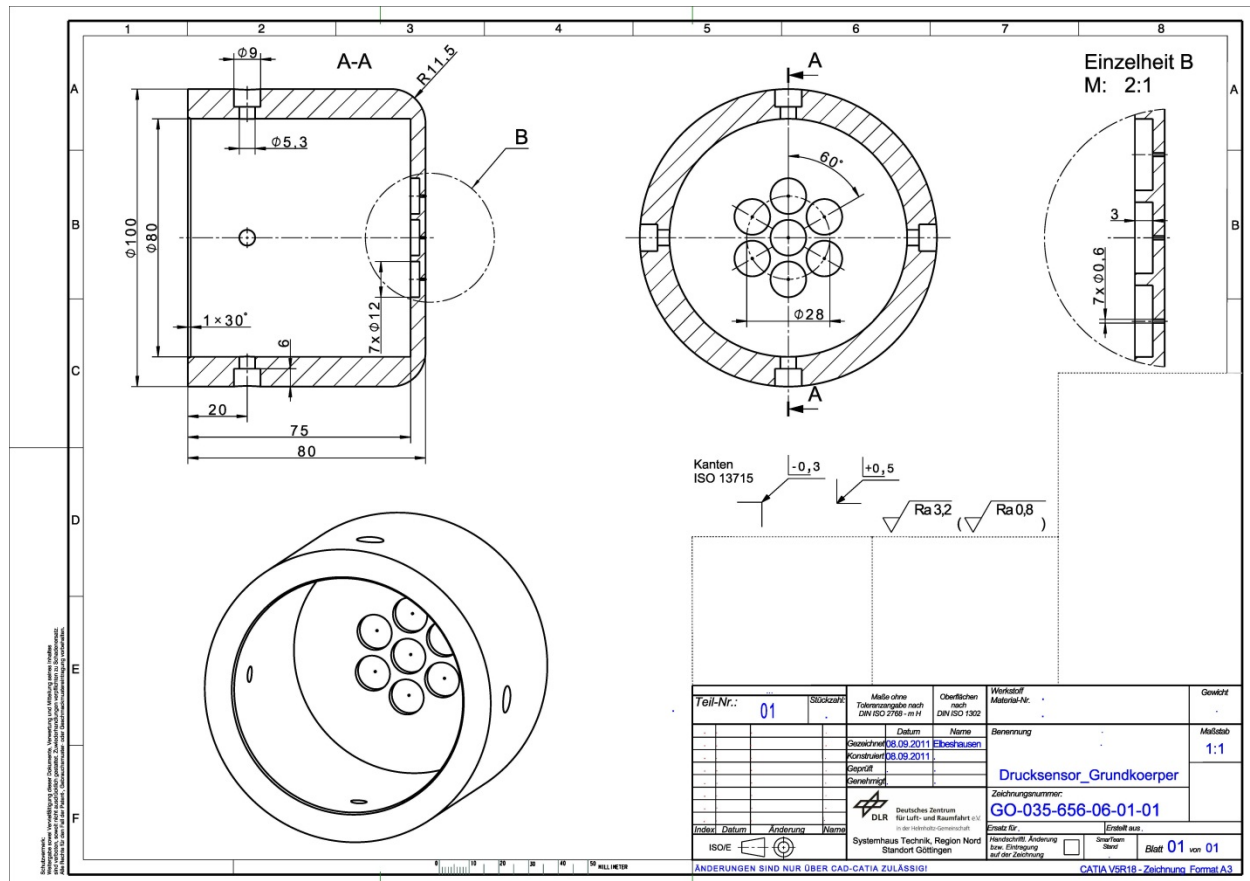


Figure 4: Technical drawing of the wind tunnel model with pressure transducer instrumentation

Photographs of the model are given in Figure 3 on page 3 and Figure 5 on page 4. Figure 3 shows on the left side the non instrumented model with a view into the inside of the body. On the right side of the figure, the model is shown after instrumentation. The pressure transducers are glued to their appropriate positions and are soldered to an electronic connection board. The connection board allows the model to be removed easily from the HEG test section in order to inspect the instrumentation in the electronic lab of HEG.



Figure 5: Photographs of the probe instrumented with thermocouples (left: outside, middle: inside, right: installed in the test section of HEG).

Figure 5 shows the heat flux probe. On the left side of the figure, the instrumented model is shown from the outside and the middle image shows the inside of the model. The technique here is the same as for the pressure probe. The thermocouples are soldered to an electronic connection board. The photograph on the right side of the image shows the model installed onto the sword in the HEG test section. All cables of the model are fed through the attachment sting and the sword out of the test section. The signals are amplified close to the test section and are then fed into the control room of HEG, where they are recorded during the run.

2.3 Instrumentation of the Model

The model is instrumented with seven pressure transducers and 10 thermocouples. The pressure transducers are installed in the stagnation point and on a constant radius of $r = 14$ mm the Table 1 on page 6 lists the angles b in degree for the pressure transducers on this constant radius. The transducer called P07 is located in the stagnation point.

Name	x [mm]	Name	r [mm]	b [°]
TL01	-10	P01	14	0
TL02	-20	P02	14	60
TR01	35	P03	14	120
TR02	30	P04	14	180
TR03	25	P05	14	240
TR04	20	P06	14	300
TR05	15	P07	0	-
TR06	10			
TR07	5			
TC01	0			

Table 1: Coordinates of the transducers installed into the model.

The thermocouples are named TL01 and TL02 for the transducers installed on one side of the stagnation point. The transducer in the stagnation point is labeled TC01. The transducers located on the other side are TR01 to TR07.

3 Experimental Setup

3.1 The High Enthalpy Shock Tunnel Göttingen (HEG)

The free piston driven shock tunnel HEG of DLR was commissioned for use in 1991 and since then it was extensively used in a large number of national and international space and hypersonic flight projects. Originally, the facility was designed for the investigation of the influence of high temperature effects such as chemical and thermal relaxation on the aerothermodynamics of entry or re-entry space vehicles. In this operating range, total specific enthalpies of up to 22 MJ/kg and nozzle stagnation pressures of up to 150 MPa can be reached. Over the last years its range of operating conditions was subsequently extended. The main emphasis was to generate new test section conditions which allow investigating the flow past hypersonic flight configurations from low altitude Mach 6 up to Mach 10 in approximately 33 km altitude ([2][3][4]). An overview of the facility details is given by the schematic and the pictures in Figure 6 on page 8. The overall length of the facility is 60 m and it weighs 280 t. Due to the resulting forces of the piston motion the whole facility moves on a rail and bearing system. Approximately a third of its weight is contributed by an inert mass which is used to reduce the tunnel recoil motion. The HEG facility consists of a secondary reservoir, a compression tube, separated from an adjoining shock tube via the primary diaphragm and a subsequent nozzle and test section. The high pressure air in the secondary reservoir drives the piston down the compression tube which is closed by a hydraulic oil system (quick disk connect) at the main diaphragm station. The shock tube is connected to the nozzle of the tunnel at the downstream closure, which is also driven by oil hydraulics to close and seal the tunnel.

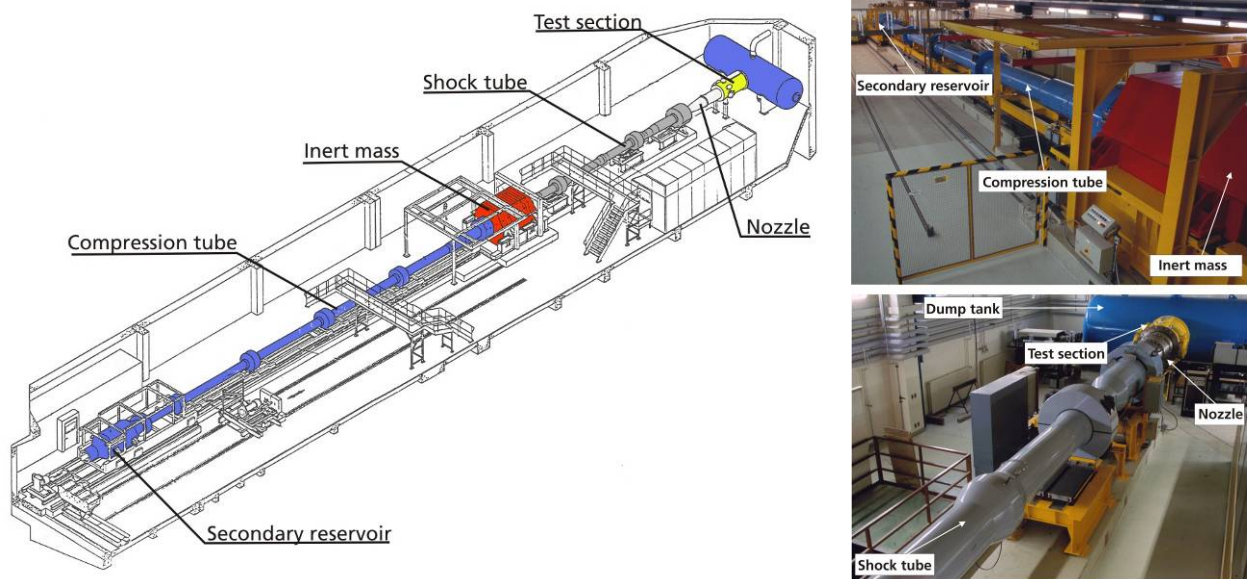


Figure 6: Schematic (left) and photographic views (right) of HEG.

For a test using a moderate enthalpy condition in HEG, a pressure of 5 MPa in the air buffer is utilized to accelerate the 280 kg piston down the 33 m long compression tube with an inner diameter of 550 mm. During this compression and heating of the driver gas, the piston reaches a maximum velocity of about 280 m/s. When the burst pressure of the 8 mm thick stainless steel main diaphragm of 48 MPa is reached, the driver gas, consisting of a helium/argon mixture, is heated up quasi-adiabatically to 4000 K. After diaphragm rupture a strong shock wave is generated. It propagates down the 17 m long shock tube (inner diameter: 150 mm) with a velocity of approximately 5 km/s and reflects from the end wall, heating up the test gas to the required reservoir conditions. Subsequently the test gas expands through a convergent-divergent contoured hypersonic nozzle with an exit diameter of 0.88 m.

3.2 Test Matrix

Two different HEG conditions have been used for the experiments. One condition is called the high pressure condition (hp) and the other one is referred to as the low pressure condition (lp) throughout this report. A total of 9 runs have been performed in HEG; all runs are listed in Table 2 given on page 9.

The hp condition has an average reservoir pressure of HEG of 53 bar, while the lp condition exhibits an reservoir pressure of 420 bar. The reservoir enthalpies are 7.842 MJ/kg and 13.67 MJ/kg, respectively. Four runs have been performed with the lp condition and five runs have been performed with the hp condition.

HEG		Modell	Condition	α	p_0 [bar]	T_0 [K]	ρ_0 [km/m ³]	h_0 [MJ/kg]
No	Run							
1	1234	hf	Lp	0°	55.76	3533	6.424	8.366
2	1235	hf	Lp	180°	54.39	3507	6.348	8.247
3	1244	hf	Hp	0°	416.4	5074	27.63	13.43
4	1245	hf	Hp	180°	411.9	5117	26.91	13.61
5	1246	hf	Hp	180°	416.3	5116	27.23	13.59
6	1247	hf	Hp	180°	406.8	5206	25.78	13.96
7	1253	p	Hp	0°	447.1	5180	28.74	13.75
8	1254	p	Lp	0°	50.27	3318	6.506	7.283
9	1255	p	Lp	0°	51.85	3357	6.571	7.471
Average	lp				53.07	3429	6.462	7.842
Dev					2.14	93	0.084	0.471
Dev(%)					4.04%	2.70%	1.30%	6.01%
Average	hp				419.7	5138	27.26	13.67
Dev					14.1	48	0.97	0.18
Dev(%)					3.37%	0.93%	3.54%	1.31%

Table 2: Test matrix of the runs performed.

Out of the four runs used with the lp condition, two runs have been performed with the model instrumented with the heat flux instrumentation (hf) and the two other runs have been performed with the pressure transducer instrumented model (p).

Additionally the model has been rotated around its axis by $\alpha = 180^\circ$, to double check the flow symmetry.

The project run numbers which are between 1 and 9, the HEG run number, the condition used and the angle of rotation of the model are listed in Table 1 given on page 6. Additionally the reservoir state of the HEG nozzle is given. At the end of Table 1, the averages of the individual runs are given. The repeatability of the runs is given in percent as well. The respectabilities are in a common range for a short time duration facility like HEG.

3.3 Free stream conditions

Two different conditions in HEG have been used for the experiments presented in this report. The low pressure condition (lp) and the high pressure condition (hp). The determination of the free stream conditions in HEG is based on a numerical reconstruction. The hypersonic nozzle is simulated with the DLR Tau Code. Specifics about this procedure can be found in [AD1].

All runs have been numerically reconstructed. The results of the computations are extracted in the flow domain from $r = 0$ mm to $r = 200$ mm. The averaged values are given in Table 3 on page 11 and Table 4 on page 12. At the end of each table, the averages of the runs are given, including the repeatability.

Run	1234	1235	1254	1255	lp averages	lp dev
x velocity	2.969E+03	2.949E+03	2.802E+03	2.832E+03	2.888E+03	2.50%
y velocity	3.542E+01	3.518E+01	3.343E+01	3.380E+01	3.446E+01	2.49%
pressure	1.473E+02	1.439E+02	1.353E+02	1.392E+02	1.414E+02	3.22%
eddy viscosity	7.251E-10	7.101E-10	6.539E-10	6.762E-10	6.913E-10	4.04%
cp	-3.618E-01	-3.618E-01	-3.618E-01	-3.618E-01	-3.618E-01	0.00%
temperature	6.822E+02	6.764E+02	6.421E+02	6.508E+02	6.629E+02	2.54%
Mach Number	6.894E+00	6.889E+00	6.830E+00	6.838E+00	6.863E+00	0.42%
viscosity	3.189E-05	3.166E-05	3.023E-05	3.058E-05	3.109E-05	2.25%
thermal conductivity	4.839E-02	4.795E-02	4.528E-02	4.595E-02	4.689E-02	2.79%
total enthalpy	6.998E+06	6.881E+06	5.997E+06	6.165E+06	6.510E+06	6.69%
ratio specific heats	1.247E+00	1.246E+00	1.241E+00	1.242E+00	1.244E+00	0.20%
CO2 mass fraction	6.977E-01	7.049E-01	7.671E-01	7.561E-01	7.314E-01	4.17%
O2 mass fraction	1.070E-01	1.046E-01	8.346E-02	8.725E-02	9.559E-02	10.84%
CO mass_fraction	1.924E-01	1.878E-01	1.482E-01	1.552E-01	1.709E-01	11.36%
C2 mass fraction	1.011E-27	1.022E-27	1.002E-27	9.925E-28	1.007E-27	1.09%
C mass fraction	1.011E-27	1.022E-27	1.002E-27	9.925E-28	1.007E-27	1.09%
O mass fraction	2.873E-03	2.662E-03	1.217E-03	1.417E-03	2.042E-03	35.86%
CO2 mole fraction	6.040E-01	6.123E-01	6.860E-01	6.728E-01	6.438E-01	5.60%
O2 mole fraction	1.275E-01	1.250E-01	1.027E-01	1.068E-01	1.155E-01	9.43%
CO mole fraction	2.617E-01	2.563E-01	2.083E-01	2.170E-01	2.359E-01	9.95%
C2 mole fraction	1.603E-27	1.627E-27	1.642E-27	1.618E-27	1.622E-27	0.88%
C mole fraction	3.206E-27	3.254E-27	3.285E-27	3.236E-27	3.245E-27	0.88%
O mole fraction	6.841E-03	6.360E-03	2.994E-03	3.467E-03	4.915E-03	34.62%
density	9.895E-04	9.782E-04	9.977E-04	1.008E-03	9.932E-04	1.08%

Table 3: Free stream conditions of the four runs performed with the lp condition. Additionally the averages and the repeatability is given at the end of each column.

Run	1244	1245	1246	1247	1253	hp averages	hp dev
x velocity	3.990E+03	4.018E+03	4.016E+03	4.073E+03	4.050E+03	4.029E+03	0.72%
y velocity	4.310E+01	4.352E+01	5.010E+01	9.873E+01	4.330E+01	5.575E+01	38.84%
pressure	1.173E+03	1.153E+03	1.168E+03	1.123E+03	1.261E+03	1.176E+03	3.91%
eddy viscosity	2.720E-09	2.658E-09	2.748E-09	2.873E-09	2.845E-09	2.769E-09	2.87%
cp	-3.607E-01	-3.607E-01	-3.607E-01	-3.608E-01	-3.606E-01	-3.607E-01	-0.01%
temperature	1.193E+03	1.196E+03	1.198E+03	1.202E+03	1.221E+03	1.202E+03	0.84%
Mach Number	6.673E+00	6.687E+00	6.683E+00	6.717E+00	6.668E+00	6.686E+00	0.25%
viscosity	4.831E-05	4.844E-05	4.849E-05	4.873E-05	4.915E-05	4.862E-05	0.61%
thermal conductivity	8.165E-02	8.186E-02	8.198E-02	8.235E-02	8.334E-02	8.224E-02	0.72%
total enthalpy	1.267E+07	1.288E+07	1.286E+07	1.330E+07	1.306E+07	1.295E+07	1.64%
ratio specific heats	1.244E+00	1.246E+00	1.245E+00	1.249E+00	1.245E+00	1.246E+00	0.15%
CO2 mass fraction	4.942E-01	4.825E-01	4.844E-01	4.604E-01	4.806E-01	4.804E-01	2.30%
O2 mass fraction	1.676E-01	1.706E-01	1.701E-01	1.759E-01	1.710E-01	1.711E-01	1.58%
CO mass_fraction	3.219E-01	3.293E-01	3.282E-01	3.434E-01	3.306E-01	3.307E-01	2.13%
C2 mass fraction	2.451E-28	2.513E-28	2.485E-28	2.622E-28	2.350E-28	2.484E-28	3.55%
C mass fraction	3.619E-27	4.433E-27	4.851E-27	7.021E-27	1.462E-26	6.909E-27	58.14%
O mass fraction	1.624E-02	1.754E-02	1.733E-02	2.022E-02	1.778E-02	1.782E-02	7.34%
CO2 mole fraction	3.876E-01	3.761E-01	3.779E-01	3.548E-01	3.743E-01	3.742E-01	2.86%
O2 mole fraction	1.808E-01	1.829E-01	1.826E-01	1.865E-01	1.832E-01	1.832E-01	1.01%
CO mole fraction	3.966E-01	4.034E-01	4.023E-01	4.158E-01	4.044E-01	4.045E-01	1.55%
C2 mole fraction	3.522E-28	3.589E-28	3.552E-28	3.702E-28	3.353E-28	3.544E-28	3.20%
C mole fraction	1.040E-26	1.266E-26	1.387E-26	1.983E-26	4.172E-26	1.970E-26	58.11%
O mole fraction	3.504E-02	3.761E-02	3.720E-02	4.286E-02	3.809E-02	3.816E-02	6.74%
density	4.080E-03	3.979E-03	4.025E-03	3.814E-03	4.256E-03	4.031E-03	3.56%

Table 4: Free stream conditions of the five runs performed with the hp condition. Additionally the averages and the repeatability is given at the end of each column

4 Experimental Measurement Techniques

4.1 Surface Pressure Measurements

Pressures on the model are measured using General Electric pressure transducers. These pressure transducers have a pressure range of 7 bar. The transducer sensitivity is sensor specific and the calibration factor of each sensor is determined including the whole measurement chain when installed in HEG. The response time of the transducers is about 7 μ s. Surface pressure measurements in short duration facilities have to use different approaches from pressure measurements in continuous running facilities. Because the measurement time is short, fast response pressure transducers have to be placed close to the surface to measure within the appropriate response times. Ten transducers in total are installed in the model (see section 2.3 on page 6).

4.2 Surface Heat Flux Measurements

Heat transfer is measured using MedTherm thermocouples. These gauges are coaxial thermocouples with a nominal response time of 1 μ s and a sensitivity of 58.8 μ V/K. The thermocouples are manufactured from chromel and constantan. The model number is TCS-061-E-XX-24-10866 where XX refers to the thermocouple length (2.54 to 22.86 mm). The thermocouples are NIST type E and have a diameter of 1.549 mm. Type E thermocouples have the highest millivolt output per degree of temperature change of all metal based thermocouples. Type E denotes the combination of chromel and constantan with chromel as the positive leg and constantan as the negative leg. Five thermocouples are installed in the model on a constant radius and one thermocouple is installed in the stagnation point coordinate of the nose of the model (see section 2.3 on page 6).

4.3 High Speed Flow Visualisation

To visualise the flow during the experiments in HEG, a high-speed flow visualization system was utilized. The system employed was a conventional Z-fold Schlieren/shadowgraph arrangement, with a pair of spherical mirrors (Halle SDH4300), having a diameter of 300 mm and a focal length of 1500 mm, to collimate the light beam and then refocus it on the imaging side. The light source used was a 1000 W short-arc Xe lamp, emitting continuous white light. A schematic of the optical setup is shown in Figure 3.7. The diameter of the visualization windows installed in the test section is 300 mm; the image magnification was controlled through the choice of focusing lens, L4. For Schlieren imaging, a razor blade (R) is positioned at the focal point of the spherical mirror H2; for flow visualization using the shadowgraph technique, the razor blade is removed and the test-section imaging plane is slightly shifted by moving lens L4, thus generating a shadowgraph effect.

For the present experiments, the images were recorded with a SHIMADZU digital camera (Model HPV-1). This camera is able to record up to 102 frames at a maximum imaging rate of 1 MHz and a fixed resolution of 312x260 pixels. For these tests, a recording rate of either 16 kHz or 32 kHz was used. As the light source was continuous, the effective exposure time was controlled by the camera shutter. The camera shutter has been set to 1/8, this means the exposure time is 1/8 of the time between two frames. The shutter of the camera remains open during the experiments. More information and details about the high speed flow visualisation system of HEG utilizing the Cordin drum camera is given in [8].

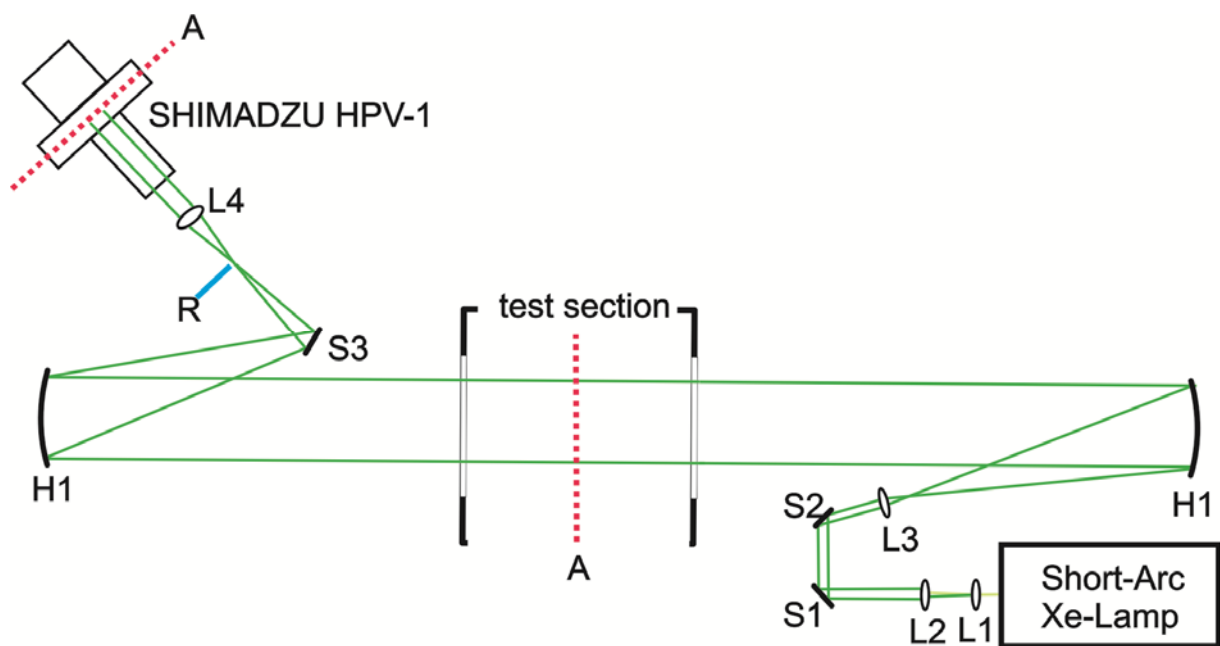


Figure 7: Schematic of the optical setup for the high speed flow visualisation. H: Parabolic mirrors, S: Plane mirrors, L: Lenses, A: Focal plane, R: Razor blade.

5 Results

This chapter will summarize all experimental results obtained during the measurements campaign in HEG. The experimental data of the surface pressure measured on the model are presented and additionally the results for the surface heat flux measurements and the results of the flow visualizations obtained during the experiments..

5.1 Surface Pressure

This section discussed the experimental results obtained for the surface pressure measurements on the model. Since the pressure profile is flat in and around the stagnation point, the pressure results are given in tabular form. Table 5 on page 16 gives the results obtained. Here all measurements are given as relative to the stagnation point transducer P07. Therefore, the result for P07 is always 1. There is no significant difference between the lp condition (Runs 1254 and 1255) and the hp condition (Run 1253). The table lists the averages of all runs on the right hand side and the averages of all measurements except the stagnation point transducer P07 blow the column. The last row shows the deviation of all transducers from the stagnation point value. It is obvious, that the deviations are smaller than the repeatability. Therefore, the pressure measurements on the probe give basically the same reading and for the comparison to the numerical simulations, it is proposed to compare to an average value of all pressure measurements.

	1253	1254	1255			
Name	p/pstag	p/pstag	p/pstag	Average	Dev	Dev[%]
P01	0.976	1.009	0.976	0.987	0.016	1.59%
P02	0.980	1.004	0.984	0.989	0.010	1.03%
P03	0.999	1.005	0.997	1.000	0.003	0.34%
P04	1.012	1.003	1.001	1.005	0.005	0.48%
P05	0.997	1.004	0.994	0.999	0.004	0.43%
P06	0.975	1.003	0.990	0.989	0.011	1.15%
P07	1	1	1	1	0	0
Average	0.990	1.005	0.990	0.995		
Dev	0.014	0.002	0.008	0.007		
Dev[%]	1.38%	0.22%	0.84%	0.67%		
1-						
Average	1.01%	-0.46%	0.97%	0.51%		

Table 5: Results of the pressure measurements.

5.2 Surface Heat Flux

This section describes the results obtained during the campaign for the surface heat flux measurements on the flaps. Because the model has been rotated around 180° , the measurements are homogeneously distributed over the surface. Figure 8 on page 17 shows the results obtained for the lp condition and the hp condition. Here, the heat flux levels are given for each individual run. Even though the data has been obtained at two different flow conditions, the normalized results are not distinguishable.

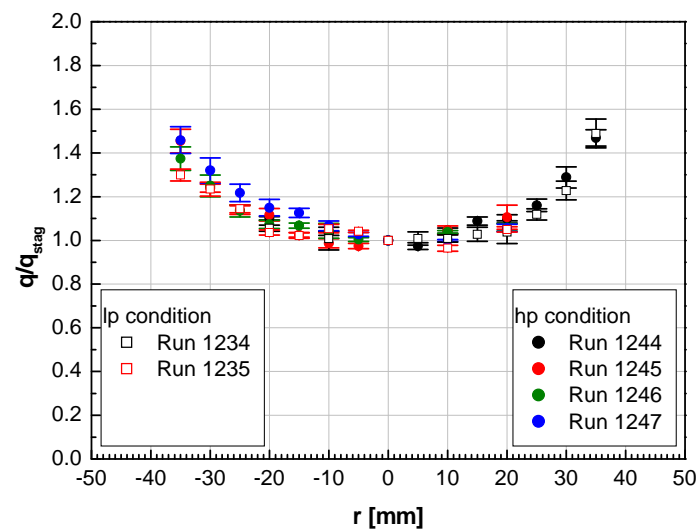


Figure 8: Results of the surface heat flux measurements for all runs..

The same trend is visible in the averaged results. Run 1234 and run 1235 have been averaged and the runs 1244, 1245, 1246 and 1247 are averaged. The data are plotted in Figure 9 on page 18. The heating level is the same for both conditions. No significant difference is obtainable from the experimental results.

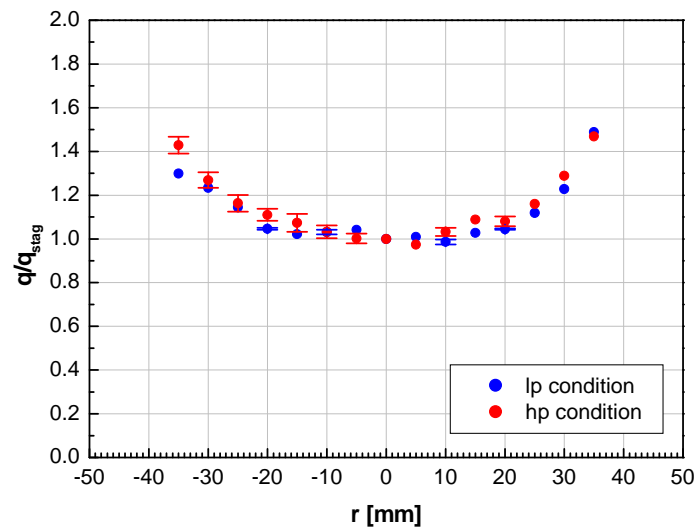


Figure 9: Results of the averaged heat flux measurements..

The next report which will be released within the SACOMAR project will give the comparisons to the numerical simulations of this test case in HEG. Then the absolute data will be compared and it might be possible to gain more insight into the flow behaviour in the shock layer and the impact on the surface heating of the probe.

5.3 Flow visualisation

This section shows briefly the flow visualizations obtained for the measurements. The Schlieren images obtained for the lp condition are given in Figure 10 on page 19. Here single images from the movies obtained during the runs 1234, 1235 and 1255 are given. The density for this condition is very low. Therefore, it was not easy to obtain good Schlieren images. The images show that with increasing sensitivity of the apparatus, the density gradients becomes better.

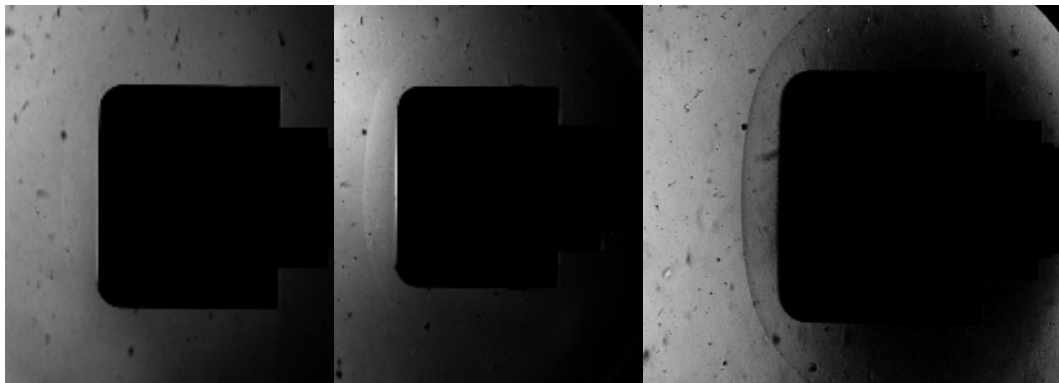


Figure 10: Experimental Schlieren images of the lp condition. The runs are from left to right: 1234, 1235 and 1255.

The images obtained for the hp condition are given in Figure 11 on page 19. Here the runs 1244, 1245 and 1247 are shown. The Schlieren quality is much better, because the density for this condition is about 4 times higher than for the lp condition.

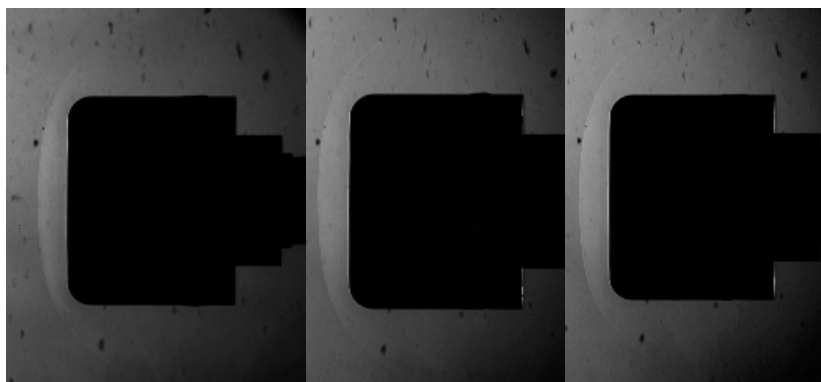


Figure 11: Experimental Schlieren images for the hp condition. The runs are from left to right: 1244, 1245, 1247.

It is hard to draw conclusions at this stage. The next report in the SCAMOR project will give the comparison between the numerical rebuilding data and the experimental data. In this context the

complete sequences will be inspected and compared to the numerical results. From this comparison, we can conclude if the shock shape and shock stand off distance will be correctly simulated by the numerical codes in this project. Also a difference in behavior between the two conditions can be detected.

6 Conclusions

Wind tunnel experiments in the High Enthalpy Shock Tunnel (HEG) of the German Aerospace Center (DLR) have been performed. The investigation was performed on cylindrical wind tunnel model, called probe. This cylindrical probe was proposed within the SCAMOR project. All experimental facilities use the same configuration for the measurements. Two model were designed and constructed. One model was instrumented with pressure transducers to determine the surface pressure and the other model was instrumented with coaxial thermocouples to determine the surface heat flux on the flap surfaces. The model is manufactured out of stainless steel

The measurements of wall pressure were reported and discussed; the same is true for the heat flux measurements. The results are consistent and the estimated errors are within acceptable bounds. The main conclusion is that the data obtained from the two different conditions used for the experimental campaign shown no significant difference, when compared in relation to the stagnation point value of the model. The flow visualizations were shown briefly to give and overview of the quality obtained. Direct conclusions cannot be drawn at this point for the shock stand off distance and shock shape.

Summarizing, it can be stated that all measurement required and demanded within the project were fulfilled.

The next report that will be delivered within the SACOMAR project will show the comparison between the experimental data obtained in HEG and the numerical data of the simulations to be performed. Then we can draw some conclusions concerning the behavior of the gas in the shock layer and the ability of the numerical simulations to reproduce this.

7 References

- [1] Hannemann, K., Martinez Schramm, J., High Enthalpy, High Pressure Short Duration Testing of Hypersonic Flows, In: Springer Handbook of Experimental Fluid Mechanics, pp.1081 – 1125, Springer Berlin Heidelberg, Eds.: Tropea, C., Foss, J., Yarin, A., 200
- [2] Hannemann, K., Schnieder, M., Reimann, B., Martinez Schramm, J., The influence and delay of driver gas contamination in HEG, AIAA 2000-2593, 21st AIAA Aerodynamic Measurement Technology and Ground Testing Conference, Denver, CO, 19-22 June, 2000
- [3] Hannemann, K., High Enthalpy Flows in the HEG Shock Tunnel: Experiment and Numerical Rebuilding, 41st AIAA Aerospace Sciences Meeting and Exhibit, 6-9 Jan, Reno, Nevada, 2003
- [4] Hannemann, K., Martinez Schramm, J., Karl, S., Recent extensions to the High Enthalpy Shock Tunnel Göttingen (HEG), Proceedings of the 2nd International ARA Days “Ten Years after ARD”, Arcachon, France, 21-23 October, 2008
- [5] McIntosh, M.K., Computer Program for the Calculation of Frozen and Equilibrium Conditions in Shock Tunnels, Australian National University, Canberra A.C.T., 1968
- [6] Reimann, B., Johnston, I., Hannemann, V., The DLR TAU-Code for High Enthalpy Flows, Notes on Numerical Fluid Mechanics and Multidisciplinary Design, Vol.87, Springer, 2004
- [7] Gupta, R.N., Yos, J.M., Thompson, R.A., Lee, K.P., A Review of Reaction Rates and Thermodynamic and Transport Properties for an 11-Species Air Model for Chemical and Thermal Nonequilibrium Calculations to 30000 K, NASA Reference Publication, No. 1232, 1990
- [8] Karl, S., Martinez-Schramm, J., Hannemann, K., High Enthalpy Cylinder Flow in HEG: A Basis for CFD Validation, AIAA 2003-4252, 33rd AIAA Fluid Dynamics Conference, Orlando, 2003

- [9] Martinez Schramm, J., Karl, S., Hannemann, K., High Speed Flow Visualization at HEG, New Results in Numerical and Experimental Fluid Mechanics IV, Springer, Editors: Breitsamter, Laschka and Heinemann, Notes on numerical fluid mechanics and multidisciplinary design, Vol. 87, pp: 229-235, 2004
- [10] Smart, M.K., Hass, N.E., Paull, A., Flight Data Analysis of the HyShot 2 Scramjet Flight Experiment, AIAA Journal, Vol.44, No.10, pp. 2366-2375, 2006
- [11] Verant, J.L., Numerical Enthalpies Rebuilding for Perfect Gas and Nonequilibrium Flows. Applications to High Enthalpy Wind-Tunnels, ONERA Report RT No. 69/6121 SY, HT-TN-E-1-201-ONER, Office National d'Études et de Recherches Aérospatiales, 1995
- [12] Schwamborn, D., Gerhold, T., Heinrich, R., The DLR TAU code: Recent Applications in Research and Industry. ECCOMAS CFD 2006, The Netherlands, 2006, TU Delft.